Parameterized nonlinear suboptimal control for tracking and rendezvous with a non-cooperative target

Dengwei Gao [a], Jianjun Luo [a,*], Weihua Ma [a], Brendan Englot [b]

[a] *School of Astronautics, Northwestern Polytechnical University, Xi'an, 710072, China*
[b] *Department of Mechanical Engineering, Stevens Institute of Technology, Hoboken, NJ, 07030, USA*

ARTICLE INFO

ABSTRACT

A specific parameterized nonlinear suboptimal control technique is proposed to control the relative position of a spacecraft in order to track a rotating target. The technique consists of using power series expansion to parameterize an SDRE (State-Dependent Riccati Equation) with an algebraic expression. One of the major contributions of this technique is the avoidance of online solution of algebraic Riccati and Lyapunov equations that will be much faster than the standard SDRE and $\theta - D$ control. Meanwhile, parameterized nonlinear suboptimal control is extended to adaptive form to verify robustness to unknown disturbances. Finally, we show two benchmark examples using this parameterized technique to construct controllers. Specifically, we also apply this technique to design the nonlinear control of a chaser spacecraft to track and rendezvous with a rotating non-cooperative target accompanied by an unknown translational maneuver. Numerical results demonstrate that the computational efficiency and tracking performance accuracy are superior to existing methods and an adaptive form is capable of offsetting unknown parameters.

© 2019 Elsevier Masson SAS. All rights reserved.

1. Introduction

State-Dependent Riccati Equation (SDRE) is a well-known method that used in the applications such as regulator design and in tracking control strategies [1]. The SDRE represents a nonlinear system using a linear-like structure by state-dependent coefficients (SDC). This control method needs to be computed at every state to obtain a nonlinear feedback controller where some defined cost function is minimized. The SDRE has emerged as a general design method which is widely used in aerospace engineering [2–5] and other fields [6].

However, the standard SDRE method needs to solve the algebraic Riccati equation (ARE) repeatedly online at every integration step to obtain the suboptimal local feedback control law, which may raise an implementation issue if dimensionality and system order are high. The article [7] proposes an approximate technique to solve the SDRE via perturbation to solve an ARE once offline and several Lyapunov equations online based on the accuracy requirement for an approximate solution. Ming Xin [8] developed an approximately closed-form feedback controller named $\theta - D$

which is also useful and extend the approximate technique in [7] for stability at large initial conditions, since it considers parameter perturbations in the state weight matrix of the cost function. Then, Ming Xin et al. [2] investigated $\theta - D$ control of a spacecraft's approach to and alignment with a tumbling target and considered the control of position and attitude in one optimal control framework. Zhang et al. [4] extended a modification term in $\theta - D$ to tracking and rendezvous with a rotating non-cooperative target with unknown translational maneuvers. Liang Sun et al. [9] proposed a gradient adaptive method to offset the parametric uncertainties of a non-cooperative spacecraft in rendezvous with model uncertainty and external disturbances. Meanwhile [10–13] showed that the adaptive method is a promising approach for solving non-cooperative target problems. Similar to the previous works, this paper proposes a new parameterized SDRE technique for speeding up online computation for designing nonlinear feedback controllers and extend it to adaptive form.

Approximations to the nonlinear regulator problem are all based upon a power series expansion of the state vector in terms of one perturbation parameter, which is an effective way to approximate the solution of the HJB and overcome computational difficulties. Especially for applications in aerospace engineering, good computational efficiency and accuracy will be very useful due to the limitations of hardware. Therefore we propose a new

Nomenclature

C_I^{bt}	transformation matrix from body-fixed frame of target to the inertial frame	$\omega_{I,bt}^I$	vector of actual angular velocity of target in inertial frame
C_I^l	transformation matrix from LOS frame to the inertial frame	r_c, r_t	state vector of chaser and target spacecrafts in inertial frame
Q, R	weight matrix on quadratic cost function	μ	gravitational constant
ρ	distance between chaser spacecraft and target		
q_ε, q_β	sight inclination and declination angle respectively	Subscripts	
n_b	required orientation in body frame of target spacecraft	0	initial variable at $t = 0$
u_c, u_t	vector of control acceleration of chaser and target spacecraft respectively	d	desired variable
		k, l	exponent index
		p, q	different parameter identification

parameterized SDRE by integrating power series expansion to an algebraic expression which is very suitable for online implementation. To compare with the traditional methods SDRE and $\theta - D$, one of the major contributions in our research is the avoidance of online solution of algebraic Riccati equations and even Lyapunov equations. Instead, the approximation in this work is used to find parameter-dependent linear control laws to stabilize a vector field at different equilibria in an appropriate region, and all the terms are computed offline. Therefore, the parameterized control law reduces the amount of online computation significantly. For non-cooperative spacecraft missions, we also studied an adaptive controller to offset the unmodeled parameters which does not significantly increase the required computation, such as unknown target maneuver. Since the algebraic expression, this suboptimal control law imposes mild restrictions, and it is asymptotically stable within a solvable region around the equilibrium which is also the range of the adaptive controller's application. Some papers have analyzed the radius of such a stable region, including [14,15].

The rest of the paper is organized as follows. The technique for the parameterized SDRE controller is presented in Section 2. Section 3 describes the properties of the proposed controller and its adaptive form. Simulation of two benchmark examples and an application in space mission are shown in Section 4 to evaluate the performance of the proposed controller. Finally, conclusions and potential applications are discussed in Sections 5 and 6.

2. Parameterized suboptimal control of an affine nonlinear system

We consider an affine nonlinear system of the form:

$$\dot{x} = f(x) + B(x)u(x) \tag{1}$$

Assume $f(x)$ is continuously differentiable. We want to find a controller for the system in Eq. (1) that minimizes the quadratic cost function given by:

$$J = \frac{1}{2} \int_0^\infty (x^T Q x + u^T R u) \mathrm{d}t \tag{2}$$

The infinite-horizon nonlinear control problem can be solved by solving a HJB partial differential equation [16].

$$\frac{\partial V^T}{\partial x} f(x) - \frac{1}{2} \frac{\partial V^T}{\partial x} B(x) R^{-1} B^T(x) \frac{\partial V}{\partial x} + \frac{1}{2} x^T Q x = 0 \tag{3}$$

where $V = \min_u J$ is the optimal cost of the above objective function (2) subject to u. After solving Eq. (3) the optimal control is

given by the solution:

$$u(x, t) = -R^{-1} B(x, t) \frac{\partial V^T}{\partial x} x(t) \tag{4}$$

Actually solving Eq. (3) is very expensive. An approximate solution of the HJB equations is parameterized by the perturbation $\epsilon \in \mathbb{R}^p$ which varies the vector field. Assuming that Eq. (1) is in the form that the dependence of system on the parameter vector ϵ and state the following:

$$\dot{x} = (A_0 + \sum_{p=1}^{\bar{p}} a_p(\epsilon) A_p) x + (B_0 + \sum_{q=1}^{\bar{q}} b_q(\epsilon) B_q) u \tag{5}$$

where A_p and B_q are both constant matrices, and a_p, b_q is a mapping of ϵ. The mappings a_p, b_q are not restricted to polynomials but any form of algebraic expression of f. $\bar{p}, \bar{q} \in \mathbb{N}$ are the upper limits allowed for parameters a_p, b_q, which is based on the form of system (1). This is the part that differs most from traditional suboptimal methods. A_0 and B_0 are both constant matrices such that (A_0, B_0) is a stabilizable pair and $(A_0 + \sum_{p=1}^{\bar{p}} a_p(\epsilon) A_p, B_0 + \sum_{q=1}^{\bar{q}} b_q(\epsilon) B_q)$ is pointwise controllable. We assume the parameterized coefficients $A(x, \epsilon) = A_0 + \sum_{p=1}^{\bar{p}} a_p(\epsilon) A_p$ and $B(x, \epsilon) = B_0 + \sum_{q=1}^{\bar{q}} b_q(\epsilon) B_q$. $(A(x, \epsilon), B(x, \epsilon))$ are treated as in an extended linearization control method, which consists of SDC like the SDRE method, leading to nonlinear control laws that render the closed-loop dynamic matrix pointwise Hurwitz.

We next assume that $L = \frac{\partial V}{\partial x}$ has a power series expansion:

$$L(x, \epsilon) = L_{0,0} + \sum_{p=1}^{\bar{p}} \sum_{q=1}^{\bar{q}} \sum_{k,l=0}^{\infty} a_p^k b_q^l L_{k,l}^{p,q} \tag{6}$$

where k, l are the exponents for each a_p, b_q, and $k + l \neq 0$. The superscript p, q of $L_{k,l}^{p,q}$ distinguishes different bases for a_p, b_q. We obtain $L(x, \epsilon) = L_{0,0}$ when $a(\epsilon) = 0, b(\epsilon) = 0$ is solving an exact Riccati equation for $L_{0,0}$:

$$A_0^T L_{0,0} + L_{0,0} A_0 - L_{0,0} B_0 R^{-1} B_0^T L_{0,0} + Q = 0 \tag{7}$$

The rest of the expansion for the a_p, b_q term $L_{k,l}^{p,q}, k < \bar{k}, l < \bar{l}$ (omitting hereafter the superscript p, q for each $L_{k,l}$) is affine in $L_{k,l}$. These are a set of Lyapunov functions:

$$(A_0 - B_0 R^{-1} B_0^T L_{0,0})^T L_{k,l} + L_{k,l}(A_0 - B_0 R^{-1} B_0^T L_{0,0})$$

$$= -L_{k-1,l} A_p - A_p^T L_{k-1,l}$$

$$+ \sum_{i=0}^{k-1}[\sum_{j=1}^{l-1} L_{i,j} B_0 R^{-1} B_0^T L_{k-i,l-j}$$

$$+ \sum_{j=0}^{l-1} L_{i,j}(B_0 R^{-1} B_q^T + B_q R^{-1} B_0^T) L_{k-i,l-j-1}$$

$$+ \sum_{j=0}^{l-2} L_{i,j} B_q R^{-1} B_q^T L_{k-i,l-j-2}] \tag{8}$$

The proof of Eq. (8) is shown in the Appendix. We note that matrix $(A_0 - B_0 R^{-1} B_0^T L_{0,0})$ is Hurwitz. The solution to Eq. (8) solves a set of Lyapunov equations that are linear terms of $L_{k,l}$ (Note: any subscripts $L_{i'<0,j'<0}$ mean that terms with $L_{i',j'}$ are nonexistent). Solving a linear Lyapunov equation is much faster than solving a Riccati equation, which is one of the main superiorities of suboptimal methods (e.g. $\theta - D$). In this paper, even these sets of Lyapunov equations can be solved offline. After parameterization the suboptimal solution can be obtained for an appropriate state space in any prescribed order of series expansion:

$$u(x, \epsilon, t) = -R^{-1} B(x) L(x, \epsilon) x(t) \tag{9}$$

If supposed that x is a function of ϵ, the control law of Eq. (9) depends only on x. If ϵ is any parameterized uncertainty, Eq. (9) will be parameterized robust SDC suboptimal control for the nonlinear system of Eq. (1).

3. Variations of the algorithm

3.1. Globally stable

For $\theta - D$ methods, the prior works have shown how to construct nonlinear control using perturbations to parameterize the terms in the cost function; the proof of convergence and stability of the $\theta - D$ methods are given in [8]. Ref. [17] explains the selection of exponential terms to diminish the terms in the cost function as time evolves.

Assume we have the closed-loop coefficient $A_{cl}(x) = A(x) - B(x)R^{-1}B(x)L(x)$. In [14] *Theorem 10*, it is shown that we could construct term $Q(x)$ in the cost function to guarantee $\dot{L} < 0$, so that the SDRE closed loop solution is (semi)globally stable.

Theorem 1. *Assume a constant control weighting R, and a state weighting $Q(x) > 0$ which are selected so that $L < 0$ for all x. Then, for any SDC parameterization of the nonlinear system which is both strongly controllable and strongly observable for all x, the SDRE closed loop solution is (semi)globally stable.*

Proof. Let $V(x)$ be the candidate Lyapunov function so that:

$$\dot{V} = x^T \dot{L} x + x^T L \dot{x} + \dot{x}^T L x = x^T(\dot{L} - Q - LBR^{-1}BL)x \tag{10}$$

Obviously, if $\dot{L} < 0$ the control will be globally stable. Thanks to build Eq. (6), we can know the algebraic expression of the quadratic Lyapunov function (10). Assume that x_d is a function of ϵ and the quadratic Lyapunov function $V = (x - x_d(\epsilon))^T L(x, x_d(\epsilon)) \times (x - x_d(\epsilon))$ along the desired trajectory can be expressed as algebraic. Then the level set $\{x \mid 0 < V(x) < \rho, \dot{V}(x) < 0\}$ represents the stable region in every local state, and $\rho = \infty$ which is globally stable.

In [14] we know $\dot{Q} < 0$ was selected so that $\dot{L} < 0$, and the system will be (semi)globally stable. Therefore, the $\theta - D$ method

provides a good way to construct a diminishing $\dot{Q}$ to expand the region of stability. So, we could also construct the parameterized $\dot{Q}$ with $D_{p,q}$ on the right side of Eq. (8), where the $D_{p,q}$ is shown as follows:

$$D_{p,q} = k_{p,q} e^{-l_{p,q}t} \{ L_{k-1,l} A_p + A_p^T L_{k-1,l}$$

$$- \sum_{i=0}^{k-1}[\sum_{j=1}^{l-1} L_{i,j} B_0 R^{-1} B_0^T L_{k-i,l-j}$$

$$+ \sum_{j=0}^{l-1} L_{i,j}(B_0 R^{-1} B_q^T + B_q R^{-1} B_0^T) L_{k-i,l-j-1}$$

$$- \sum_{j=0}^{l-2} L_{i,j} B_q R^{-1} B_q^T L_{k-i,l-j-2}]\} = 0 \tag{11}$$

Solving Eq. (8) is an offline calculation so that the time in (11) should use a prior estimated value that is increasing monotonically. However, tuning the parameters of $k_{p,q}$ and $l_{p,q}$ in the term $D_{p,q}$ is not quantitative, since $\dot{L}$ in (10) cannot be obtained in $\theta - D$ or SDRE methods explicitly. To use Eq. (6) we can compute an algebraic expression for the quadratic Lyapunov function $V(x) = x^T Lx$. Therefore we can know the convergence properties of each trajectory by the algebraic control law (9). □

3.2. Adaptive control

Model-based control design techniques are limited by inaccurate models of the plant dynamics and even some terms that cannot be modeled like the unknown maneuvering of a target. Adaptive controllers have emerged as powerful solutions for handling unknown parameters. Following [18] and [19], we consider a system with unknown parameter θ:

$$\dot{x} = f(x) + B(x)u_\theta + F(x)\theta \tag{12}$$

with $\theta \in \mathbb{R}^r$. The mappings $f(x)$, $B(x)$ and $F(x)$ are smooth, and $f(0) = 0$, $F(0) = 0$. We search for an adaptive controller u_θ and an estimate of unknown parameters θ for system (12). Let us assume the following estimation of unknown parameters:

$$\dot{\hat{\theta}} = \tau(x, \hat{\theta}) \tag{13}$$

Using the above analysis we have an algebraic expression of the quadratic Lyapunov function $V(x)$, which is a smooth, positive-definite, scalar function. Now consider a candidate Lyapunov function for this system:

$$V_\theta = V(x) + \frac{1}{2}\tilde{\theta}^T \Gamma \tilde{\theta} \tag{14}$$

where $\tilde{\theta} = \theta - \hat{\theta}$ and user-defined matrix $\Gamma = \Gamma^T > 0$. If we let:

$$\dot{\hat{\theta}} = \tau(x, \hat{\theta}) = -\Gamma^{-1} F(x)^T (\frac{\partial V}{\partial x})^T \tag{15}$$

The time derivative of this candidate Lyapunov function is:

$$\dot{V}_\theta = \frac{\partial V}{\partial x} + \tilde{\theta}^T \Gamma \dot{\tilde{\theta}} = \frac{\partial V}{\partial x}(f(x) + F(x)\theta + B(x)u_\theta) + \tilde{\theta}\Gamma\tau(x, \hat{\theta}) \tag{16}$$

which takes the form:

$$\dot{V}_\theta = \frac{\partial V}{\partial x}[f(x) + F(x)\hat{\theta} + B(x)u_\theta] \tag{17}$$

Thus, if we find the adaptive control law u_θ such that $\dot{V}_\theta < 0, \forall x, \theta, \hat{\theta}$, then we have an adaptive control law u_θ in an invariant
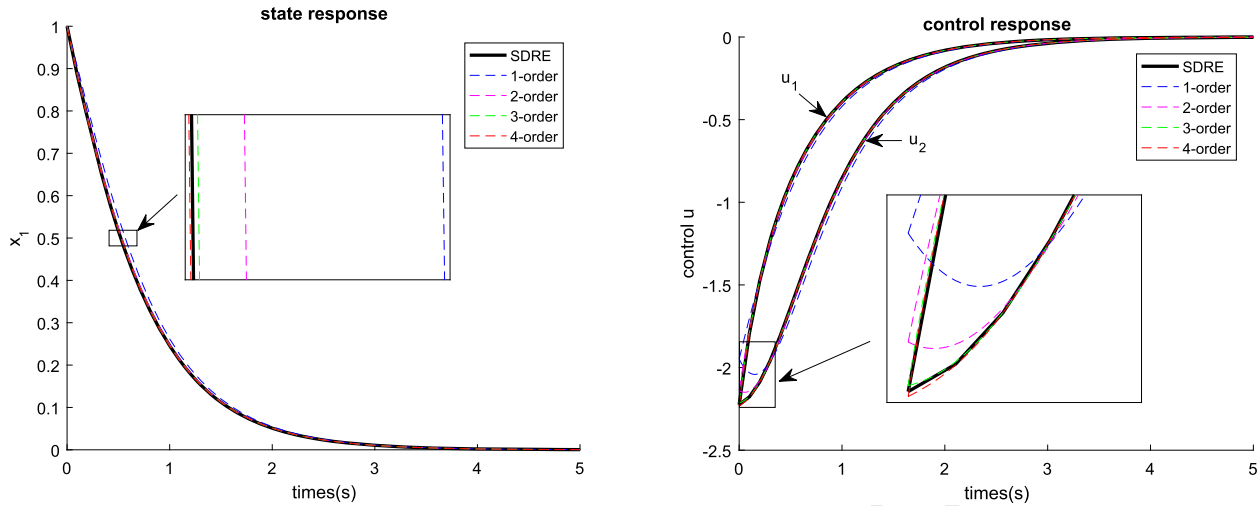
Fig. 1. 2-D benchmark problem: $\boldsymbol{x}_0 = [1, 1]^T$. Solid black curve is the result of the standard SDRE method; different colors of dashed curves represent different order expansions in our method. (For interpretation of the colors in the figure(s), the reader is referred to the web version of this article.)

region which guarantees that $\boldsymbol{x} \to 0$ as $t \to \infty$. Thus we parameterize the adaptive controller as:

$$\boldsymbol{u}_\theta = \boldsymbol{u}_{par} + \boldsymbol{K}_\theta \hat{\boldsymbol{\theta}} \tag{18}$$

where $\boldsymbol{u}_{par}$ comes from Eq. (9), and $\boldsymbol{K}_\theta \hat{\boldsymbol{\theta}}$ is the adaptive modified term, where we choose $\boldsymbol{K}_\theta = -\boldsymbol{B}^L \boldsymbol{F}(\boldsymbol{x})$ (where $\boldsymbol{B}^L$ that satisfies $\boldsymbol{B}\boldsymbol{B}^L = \boldsymbol{I}$ is the left inverse of $\boldsymbol{B}$). So the closed-loop system will be:

$$\dot{\boldsymbol{x}} = \boldsymbol{A}_{cl}(\boldsymbol{x})(\boldsymbol{x} - \boldsymbol{x}_d) + \boldsymbol{F}(\boldsymbol{x})(\theta - \hat{\theta}) \tag{19}$$

Obviously, Eq. (19) is a stable system. In addition, combining the outcomes of the Subsections 3.1 and 3.2, we can achieve an adaptive control in a large stable region to offset unknown terms due to solution of algebraic expression.

4. Simulation

First we use two simple benchmark examples in Subsections 4.1 and 4.2 to test the capabilities of our methods, and in Subsection 4.3 we simulate the spacecraft relative position control to track and rendezvous with a rotating non-cooperative target with an unknown orbit maneuver.

4.1. Constant B(x) matrix example

We wish to find a control $\boldsymbol{u}$ to minimize the cost function and drive the system to the origin ($\boldsymbol{x}_d = \boldsymbol{0}$), which is from the formulation given in Section 2.4 in [8]:

$$J = \frac{1}{2} \int_0^\infty (\boldsymbol{x}^T \begin{bmatrix} 1 & 0 \\ 0 & 1 \end{bmatrix} \boldsymbol{x} + \boldsymbol{u}^T \begin{bmatrix} 2 & 0 \\ 0 & 2 \end{bmatrix} \boldsymbol{u}) dt \tag{20}$$

Assume $\boldsymbol{x} = [x_1, x_2]^T$, and $\boldsymbol{u} = [u_1, u_2]^T$ so that the system is defined by:

$$\dot{x}_1 = x_1 - x_1^3 + x_2 + u_1$$
$$\dot{x}_2 = x_1 + x_1^2 x_2 - x_2 + u_2 \tag{21}$$

For this problem, $\boldsymbol{f}(\boldsymbol{x})$ is factorized using SDC with parameterized form:

$$\boldsymbol{A}(\boldsymbol{x}) = \begin{bmatrix} 1 & 1 \\ 1 & -1 \end{bmatrix} + x_1^2 \begin{bmatrix} -1 & 0 \\ 0 & 1 \end{bmatrix}, \boldsymbol{B}_0 = \begin{bmatrix} 1 \\ 1 \end{bmatrix} \tag{22}$$

For analysis, the results are compared with the standard SDRE method.

x_1 is close to x_2 so that we only show the plot of the state response of x_1 in the state response subfigure of Fig. 1. It is evident from the zoomed-in view of the of state response subfigure that higher order leads to better performance, which is close to the result of standard SDRE. The control response subfigure shows the same phenomenon, since a better approximation is achieved at a higher order. The two sets of curves shown are u_1 and u_2 versus time.

From the above simulation, it is clear that the second order result achieved a sufficient accuracy to approach the SDRE result. Thus in the following we use second order parameterized control to design an adaptive controller. We assume the system (21) has an unknown constant scalar uncertainty $\theta = 1$ and the coefficient $\boldsymbol{F}(\boldsymbol{x}) = [1, 1]^T$. Thus the real system is as follows:

$$\dot{x}_1 = x_1 - x_1^3 + x_2 + 1 + u_1$$
$$\dot{x}_2 = x_1 + x_1^2 x_2 - x_2 + 1 + u_2 \tag{23}$$

However, in the modeled system, θ is an unknown the parameter which was specifically set to zero as an initial guess: $\hat{\theta} = 0$. In the first iteration, we also choose $V_\theta = V$ which is a valid Lyapunov function with the robustness in the stable region. In the analyses of Subsection 3.1, we can check the capacity to converge with unknown parameter θ and give an initial state using level-set computation. The robustness analysis is discussed in [14]. The weight matrix for θ in the Lyapunov function is set as $\boldsymbol{\Gamma} = \text{diag}([10, 10])$. The state and control responses are shown in Fig. 2. The simulation time is shown over a period of 10 s.

The results can be seen in Figs. 2 and 3. It is clear in the state response of Fig. 2 that if there are unknown parameters in the real system that we have not been modeled, then the state response fails to converge to zero (black curve), while the adaptive one does (red curve). Meanwhile, the estimated parameter does converge to the true parameter $\hat{\theta} \to \theta$, which is shown in Fig. 3 (black curve).

4.2. State dependent B(x) matrix example

Assume $\boldsymbol{x} = [x_1, x_2]^T$. We wish to find a control law $\boldsymbol{u}$ to minimize the following cost function, which is from section 2.5 in [8]:

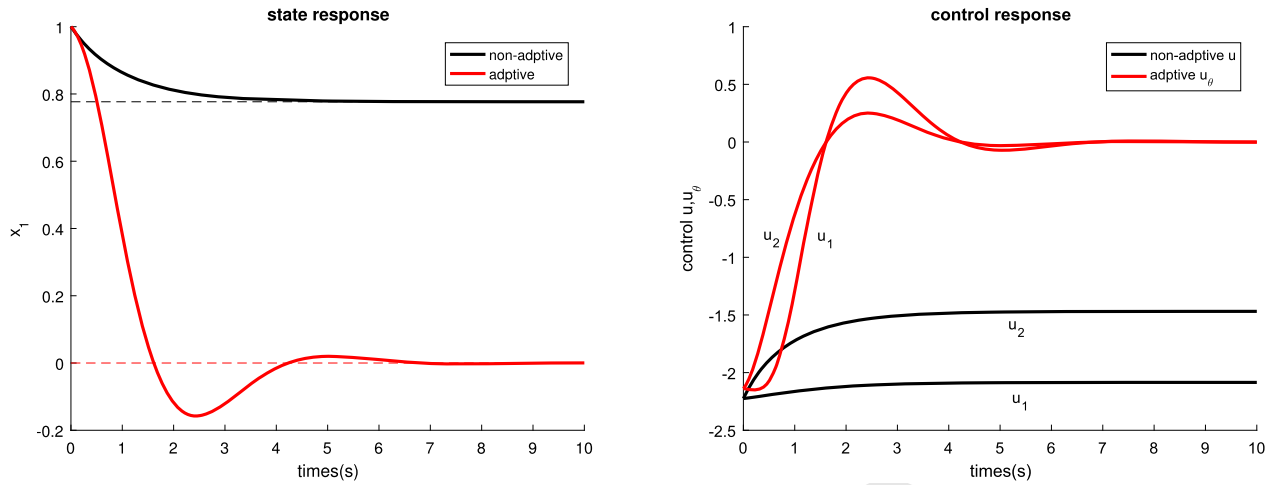$$J = \frac{1}{2} \int_0^\infty (x_1^2 + 2x_2^2 + u^2) dt \tag{24}$$

Fig. 2. 2-D benchmark adaptive problem: $\boldsymbol{x}_0 = [1 \quad 1]^T$. The black curves are the result of non-adaptive control and the red curves represent the result of adaptive control. The red dashed line is the location of the final equilibrium.
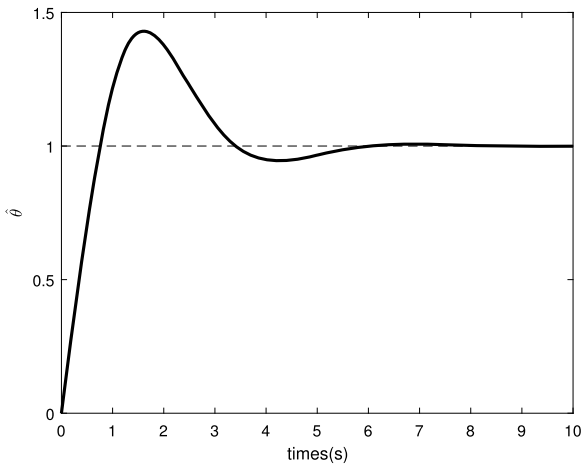

Fig. 3. $\hat{\theta}$ versus time.

with system dynamics described by:

$$\begin{aligned}\dot{x}_1 &= x_2 + (x_1 - 1)u \\ \dot{x}_2 &= x_1 + x_2 - (x_1 + 2)u\end{aligned} \tag{25}$$

The SDC are selected as:

$$\boldsymbol{A_0} = \begin{bmatrix} 0 & 1 \\ 1 & 1 \end{bmatrix}, \boldsymbol{B(x)} = \begin{bmatrix} -1 \\ -2 \end{bmatrix} + x_1 \begin{bmatrix} 0 \\ -1 \end{bmatrix} + x_2 \begin{bmatrix} 1 \\ 0 \end{bmatrix} \tag{26}$$

Simulation results are shown in Fig. 4. We obtain the same conclusion as the first benchmark example. Higher order expansion will obtain better approximations of SDRE optimal control. The control could be expressed as a polynomial in the appropriate region. These two benchmark examples also show that the relatively poor approximation of control is due to the error between the current state and the origin of expansion. Hence the power series approximation could be useful in tracking problems which are not far away from the nominal trajectory or the desired equilibrium point.

4.3. Tracking and rendezvous with a rotating non-cooperative target

In this simulation, we consider the spacecraft mission performing a track and rendezvous with a non-cooperative target such as space debris or a disabled satellite. In order to verify our parameterized controller, the simulations separate to two cases: a rotating non-cooperative target without translational maneuvers and a ro-
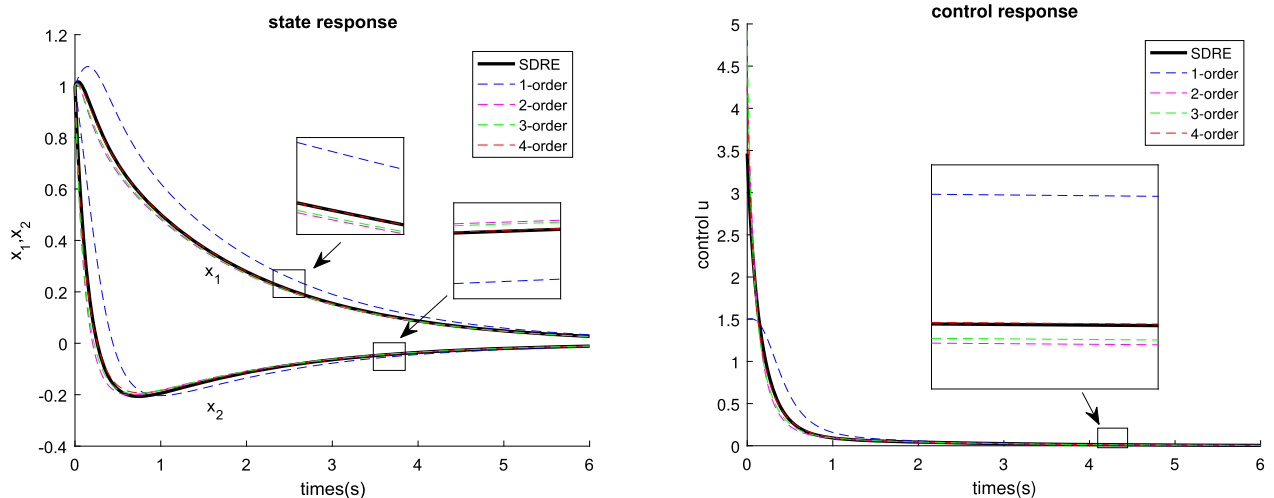

Fig. 4. 2-D benchmark problem with state-dependent $\boldsymbol{B(x)}: \boldsymbol{x}_0 = [1; 1]$.
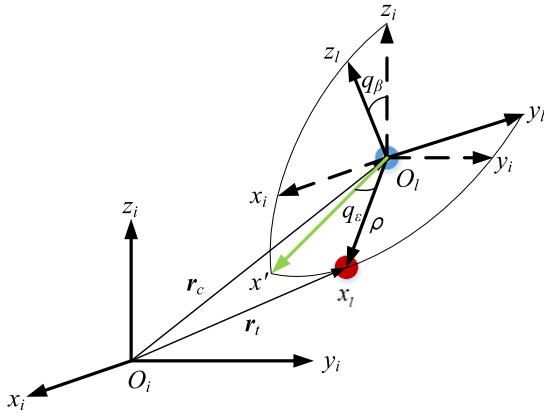
Fig. 5. LOS frame: O_i is the mass center of the earth and O_l is the center of the center of mass of the chaser spacecraft. The blue and red spheres represent the chaser and target spacecraft respectively.

tating non-cooperative target with an unknown translational maneuvers. In first case, we use our parameterized controller without adaptive modification and compare with SDRE and $\theta - D$ controller. In second case, a unknown translational maneuvers of the rotating non-cooperative is considered in the mission. The parameterized controller with adaptive modification is used to track and rendezvous with the non-cooperative target.

The spacecraft kinematics and dynamics neglecting the gravity difference in the LOS frame can be described by [4], and we add the gravity difference item to complete the model. This relative dynamic model built in the LOS frame is widely used in missile missions to deal with maneuver targets. For a non-cooperative target in space, the relative motion equations are built in the LOS frame with the origin at the center of mass of the chaser spacecraft to avoid introducing unknown parameters into the equation.

As shown in Fig. 5, $O_i x_i y_i z_i$ represents an inertial frame that is fixed to the center of the Earth. By making use of transformation via coordinate translation, $O_i x_i y_i z_i$ is used to obtain the dashed line coordinate system which is fixed at the center of mass of the chaser spacecraft. $O_l x_l y_l z_l$ represents the Line-of-Sight frame (LOS frame) that is also fixed to the center of mass of the chaser. The sight inclination and declination angles $q_\varepsilon \in (-\frac{\pi}{2}, \frac{\pi}{2})$, $q_\beta \in (-\pi, \pi)$ are generated by the coordinate rotation of $O_l x_i y_i z_i$ and transition coordinate $O_l x' y_i z_l$ which are shown in Fig. 5. ρ is the distance between chaser and target spacecraft. The dynamic equations are shown as follows:

$$
\begin{cases}
\ddot{\rho} - \rho \left(\dot{q}_\varepsilon^2 + \dot{q}_\beta^2 \cos^2 q_\varepsilon \right) = \Delta g_x + u_{tx} - u_{cx} \\
\rho \ddot{q}_\varepsilon + 2\dot{\rho}\dot{q}_\varepsilon + \rho \dot{q}_\beta^2 \sin q_\varepsilon \cos q_\varepsilon = \Delta g_y + u_{ty} - u_{cy} \\
- \rho \ddot{q}_\beta \cos q_\varepsilon + 2\rho \dot{q}_\beta \dot{q}_\varepsilon \sin q_\varepsilon - 2\dot{\rho}\dot{q}_\beta \cos q_\varepsilon \\
\quad = \Delta g_z + u_{tz} - u_{cz}
\end{cases}
\tag{27}
$$

The first and last equations in Eq. (27) describe relative longitudinal movement of the sight direction and transverse movement of the sight angle respectively. These dynamic equations in LOS coordinates could be applied to any relative motion form of orbit. In state-space, assume $\boldsymbol{x} = [\rho, q_\varepsilon, q_\beta, \dot{\rho}, \rho \dot{q}_\varepsilon, \rho \dot{q}_\beta \cos q_\varepsilon]^T$ represents our state vector so that the dynamic model can be expressed as a nonlinear system in state space:

$$
\begin{cases}
\dot{x}_1 = x_4 \\
\dot{x}_2 = x_5/x_1 \\
\dot{x}_3 = x_6/(x_1 \cos x_2) \\
\dot{x}_4 = (x_5^2 + x_6^2)/x_1 + \Delta g_x + u_{tx} - u_{cx} \\
\dot{x}_5 = -x_4 x_5/x_1 - x_6^2 \sin x_2/(x_1 \cos x_2) + \Delta g_y + u_{ty} - u_{cy} \\
\dot{x}_6 = -x_4 x_6/x_1 + x_5 x_6 \sin x_2/(x_1 \cos x_2) - \Delta g_z - u_{tz} + u_{cz}
\end{cases}
\tag{28}
$$

where the gravity difference in the LOS frame (identified by superscript l, and omitted in this article) $\Delta \boldsymbol{g} = [\Delta g_x, \Delta g_y, \Delta g_z]^T$; $\boldsymbol{u}_t = [u_{tx}, u_{ty}, u_{tz}]^T$ and $\boldsymbol{u}_c = [u_{cx}, u_{cy}, u_{cz}]^T$ represent the acceleration of target and chaser spacecraft respectively. The gravity difference in the inertial frame (identified by superscript I) can be expressed as follows:

$$
\Delta \boldsymbol{g}^I = \frac{\mu}{r_c^3} \boldsymbol{r}_c - \frac{\mu}{r_t^3} \boldsymbol{r}_t
\tag{29}
$$

We assume $\boldsymbol{\rho}^I = \boldsymbol{r}_t - \boldsymbol{r}_c$. Since $r_c = \|\boldsymbol{r}_c\| \gg \rho = \|\boldsymbol{\rho}^I\|$, $r_t = \|\boldsymbol{r}_t\| \gg \rho$, the gravity difference can be expressed as a first order approximation of the Taylor expansion at $\boldsymbol{r}_c$:

$$
\Delta \boldsymbol{g}^I = \frac{\mu}{r_c^3} [\boldsymbol{\rho}^I - \frac{3}{r_c^2} (\boldsymbol{r}_c \cdot \boldsymbol{\rho}^I) \boldsymbol{r}_c]
\tag{30}
$$

The gravity difference is linear in $\boldsymbol{\rho}^I$. For simplification, we first design a model-based open-loop control to offset the gravity difference: $\boldsymbol{u}_{offset} = -\Delta \boldsymbol{g} = -\boldsymbol{C}_l^I \Delta \boldsymbol{g}^I$ where $\boldsymbol{C}_l^I$ is the transformation matrix from inertial frame to LOS frame, $\boldsymbol{C}_l^I = (\boldsymbol{C}_I^l)^T$:

$$
\boldsymbol{C}_l^I = \boldsymbol{C}_z(q_\varepsilon) \boldsymbol{C}_y(q_\beta) = \begin{bmatrix} \cos q_\varepsilon \cos q_\beta & \sin q_\varepsilon & -\cos q_\varepsilon \sin q_\beta \\ -\sin q_\varepsilon \cos q_\beta & \cos q_\varepsilon & \sin q_\varepsilon \sin q_\beta \\ \sin q_\beta & 0 & \cos q_\beta \end{bmatrix}
\tag{31}
$$

In space operation tasks with non-cooperative targets, we note that a specified orientation in the body frame of the target is necessary for subsequent tasks like docking. Assume $\boldsymbol{n}_b$ contains the prescribed orientation in the body frame of the target spacecraft, so that $-\boldsymbol{n}_b$ is the desired direction of LOS tracking. Then, the desired direction is projected into the inertial frame:

$$
\boldsymbol{\rho}_d^I = \boldsymbol{C}_I^{bt}(-\boldsymbol{n}_b \rho_d)
\tag{32}
$$

The desired position in the LOS frame is $\boldsymbol{\rho}_d = [\rho_d, 0, 0]^T$. The desired distance between the chaser and the target ρ_d is projected into the inertial frame:

$$
\begin{aligned}
\boldsymbol{\rho}_d^I &= \boldsymbol{C}_I^l \boldsymbol{\rho}_d \\
\dot{\boldsymbol{\rho}}_d^I &= (\boldsymbol{\omega}_{I,bt}^I)^\times \boldsymbol{\rho}_d^I
\end{aligned}
\tag{33}
$$

Eq. (32) and Eq. (33) can deduce the desired sight inclination and declination angles: $q_{\varepsilon,d}, q_{\beta,d}$ and $\dot{q}_{\varepsilon,d}, \dot{q}_{\beta,d}$.

The simulation is developed to test the performance of the proposed parameterized method in the translational control of the chaser spacecraft. The mass of the chaser is 100 kg. In order to compare the performances of different control methods, the control accelerations are not limited in the saturator, but we choose the appropriate parameters $\boldsymbol{Q}$ and $\boldsymbol{R}$ that let the control accelerations along each axis are less than 0.05 (m/s^2). The initial orbit parameters of the chaser and target spacecrafts are given in Table 1.

The target is rotating with an angular velocity $\omega = 0.1°/s$ at axis $[1, 1, 1]^T$ in its body frame. The initial quaternion of the target attitude is: $q_t = [0.7071, -0.3126, 0.5477, -0.3162]^T$.

Table 1

Orbit parameters of the chaser and target.

Orbit parameters	Target	Chaser
Eccentricity	0.01	0.01
Inclination (deg)	50.002	50.002
Right ascension of ascending node (deg)	9.9981	9.9981
Semimajor axis (km)	8000	8000
Argument of perigee (deg)	30.1	30.0001
Initial true anomaly (deg)	111.0736	111.0679
μ (m^3/s^2)	3.9860044 $\times 10^{14}$	
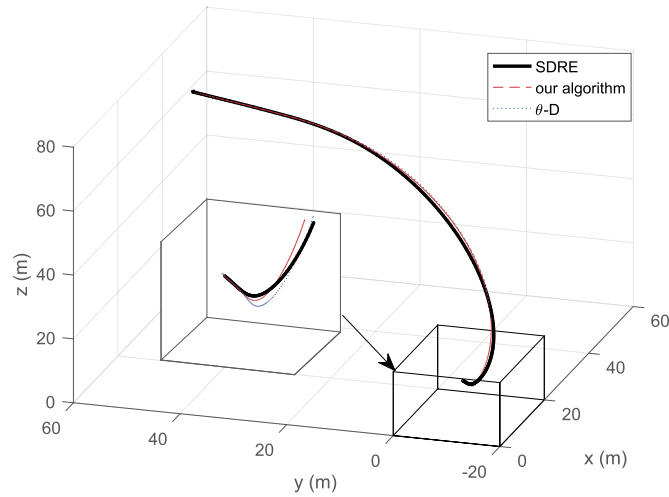
Fig. 6. 3D Trajectory in $O_i x_i y_i z_i$ frame.

We seek a control $\boldsymbol{u}$ with control cost weight matrices: $\boldsymbol{Q} =$ diag([0.01, 1000, 1000, 1, 1000, 10000]), $\boldsymbol{R} =$ diag([1000, 10000, 100]). The dynamic model is shown in Eq. (27). The parameters for $\theta - D$ are selected in the same. We selected the SDC as (omitting the subscript d):

$$\boldsymbol{A}_0 = \begin{bmatrix} 0 & 0 & 0 & 1 & 0 & 0 \\ 0 & 0 & 0 & 0 & 1/\rho_0 & 0 \\ 0 & 0 & 0 & 0 & 0 & 1/(\rho_0 \cos q_{\varepsilon 0}) \\ 0 & 0 & 0 & 0 & \dot{q}_{\varepsilon 0} & \dot{q}_{\beta 0} \cos q_{\varepsilon 0} \\ 0 & 0 & 0 & -\dot{q}_{\varepsilon 0} & 0 & -\dot{q}_{\beta 0} \sin q_{\varepsilon 0} \\ 0 & 0 & 0 & -\dot{q}_{\beta 0} \cos q_{\varepsilon 0} & \dot{q}_{\beta 0} \sin q_{\varepsilon 0} & 0 \end{bmatrix} \quad (34)$$

$$\boldsymbol{A}(\boldsymbol{x}) = \boldsymbol{A}_0 + a_1 \begin{bmatrix} \boldsymbol{0}_{2\times 4} & \boldsymbol{\Psi}_1 \\ \boldsymbol{0}_{4\times 4} & \boldsymbol{0}_{4\times 2} \end{bmatrix} + a_2 \begin{bmatrix} \boldsymbol{0}_{2\times 5} & \boldsymbol{0}_{2\times 1} \\ \boldsymbol{0}_{4\times 5} & \boldsymbol{\Psi}_2 \end{bmatrix}$$
$$+ a_3 \begin{bmatrix} \boldsymbol{0}_{3\times 3} & \boldsymbol{0}_{3\times 3} \\ \boldsymbol{0}_{3\times 3} & \boldsymbol{\Psi}_3 \end{bmatrix} + a_4 \begin{bmatrix} \boldsymbol{0}_{3\times 3} & \boldsymbol{0}_{3\times 3} \\ \boldsymbol{0}_{3\times 3} & \boldsymbol{\Psi}_4 \end{bmatrix} \quad (35)$$
$$+ a_5 \begin{bmatrix} \boldsymbol{0}_{4\times 4} & \boldsymbol{0}_{4\times 2} \\ \boldsymbol{0}_{2\times 4} & \boldsymbol{\Psi}_5 \end{bmatrix}$$

where $a_1 = 1/x_1 - 1/\rho_0$, $a_2 = 1/x_1/\cos x_2 - 1/(\rho_0 \cos q_{\varepsilon 0})$, $a_3 = x_5/x_1 - \dot{q}_{\varepsilon 0}$, $a_4 = x_6/x_1 + \dot{q}_{\beta 0} \sin q_{\varepsilon 0}$, $a_5 = x_6 \sin x_2/(x_1 \cos x_2) - \dot{q}_{\beta 0} \sin q_{\varepsilon 0}$. $\boldsymbol{\Psi}_1 = \begin{bmatrix} 0 & 0 \\ 1 & 0 \end{bmatrix}$, $\boldsymbol{\Psi}_2 = [1, 0, 0, 0]^T$, $\boldsymbol{\Psi}_3 = \begin{bmatrix} 0 & 1 & 0 \\ -1 & 0 & 0 \\ 0 & 0 & 0 \end{bmatrix}$, $\boldsymbol{\Psi}_4 = \begin{bmatrix} 0 & 0 & 1 \\ 0 & 0 & 0 \\ -1 & 0 & 0 \end{bmatrix}$, $\boldsymbol{\Psi}_5 = \begin{bmatrix} 0 & -1 \\ 1 & 0 \end{bmatrix}$.

Fig. 6 and Fig. 7 provide a numerical comparison of the SDRE (solid black), our algorithm (dashed red) and the $\theta - D$ algorithm (dotted blue). The expansion order of our algorithm and the $\theta - D$
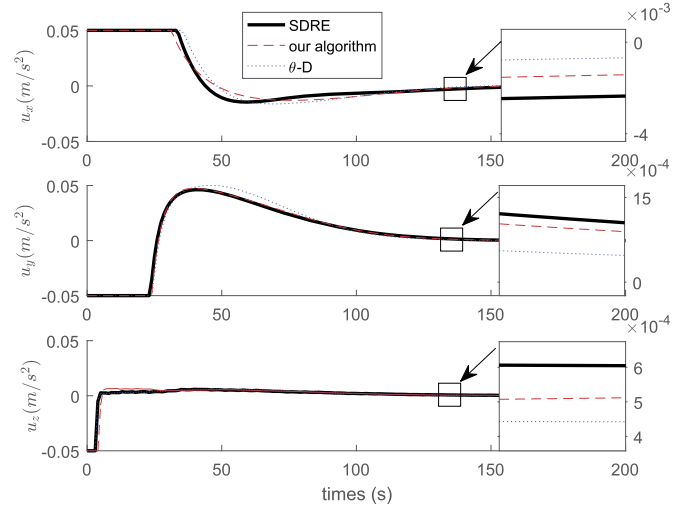

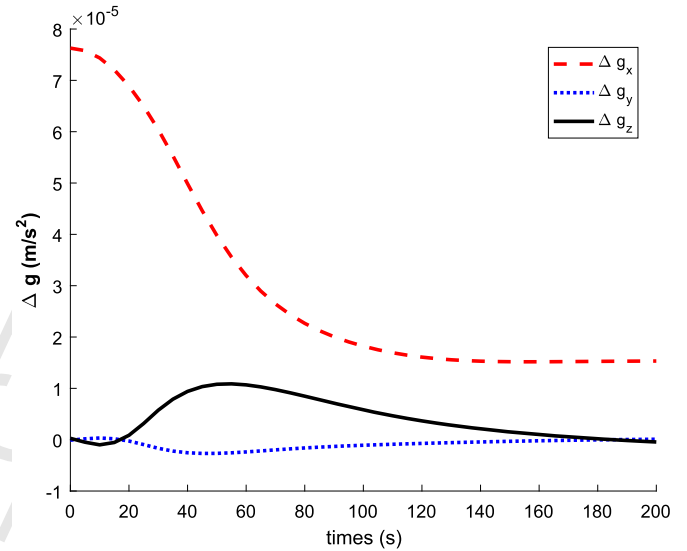**Fig. 7.** Control acceleration.

Fig. 8. Gravity difference in LOS frame.

algorithm are both 2nd order at the initial position. We set the initial position of the chaser as shown in Table 1, when there is no target orbit maneuver to influence the relative motion. The simulation shows the approach and flight process around the chaser, seen in Fig. 6, which is a plot of 3D relative trajectory in the inertial frame and computed by Eq. (33). The two approximate methods have a similar control precision. The control acceleration of the chaser spacecraft is shown in Fig. 7, where we can see similar control precision with the $\theta - D$ algorithm of the same order. The control law shown in Fig. 7 is designed using the model of Eq. (28) without considering the gravity difference. This numerical simulation in Fig. 8 shows the gravity difference during 100 s. This is much smaller than the control acceleration and we can also use an additional control to offset its effects. Fig. 9 shows the time complexity for this problem after normalization with SDRE in first to fourth order expansions in the same numerical simulation with the same simulation environment (CPU i7-6700HQ, RAM 8 GB, Matlab R2016a). Obviously, our algorithm is much faster than SDRE and $\theta - D$ algorithm.

For target maneuvering case, we use the adaptive controller described in Section 3.2 to control the incomplete modeled system in Eq. (28) with $\boldsymbol{u}_t \neq 0$ and unknown. From the previous simulations,
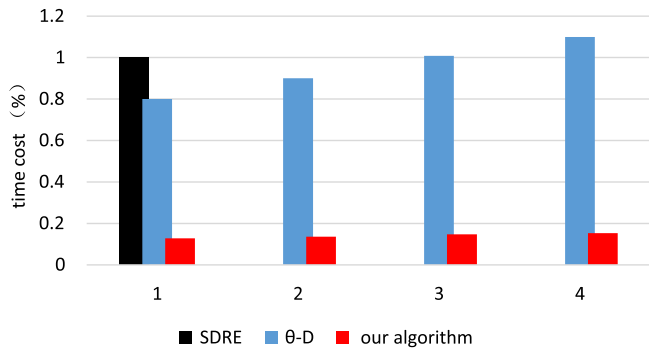
Fig. 9. Computation time cost.
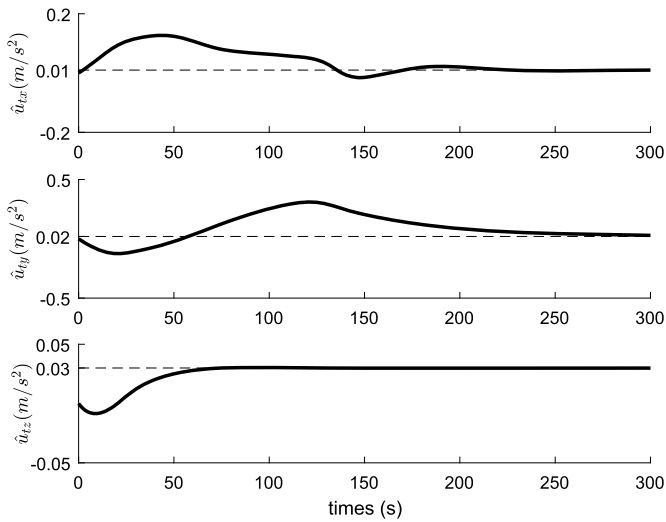

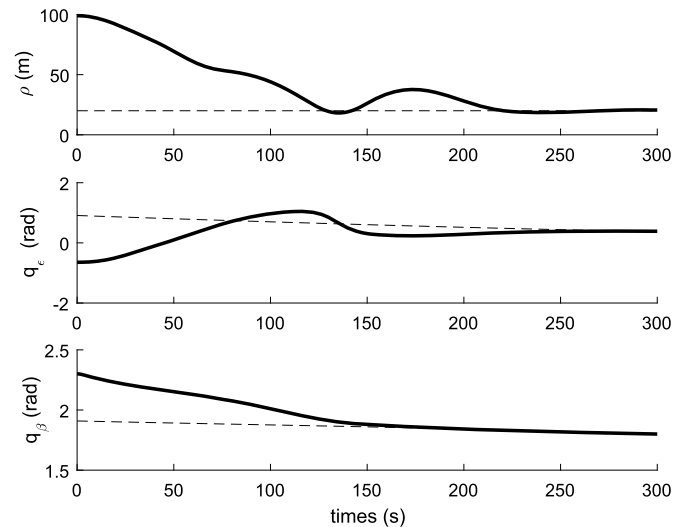**Fig. 10.** Estimated maneuvering of target with time.
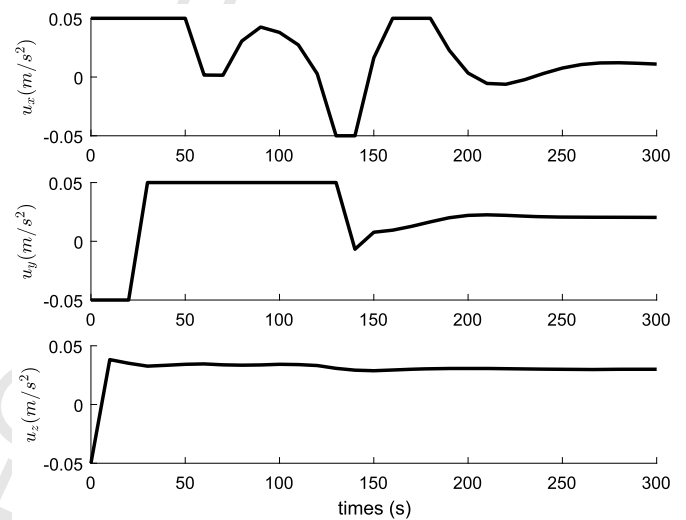

Fig. 11. Main states with time.

Fig. 12. Adaptive control acceleration.

we notice that adaptive control provides an offset between the modeled system and the true system. Hence if the target spacecraft has an unknown maneuver acceleration $\boldsymbol{u}_t$, it is assumed to be a constant $\boldsymbol{u}_t = [0.01, \ 0.02, \ 0.03]^T$ m/s² in simulation. To test our algorithm, the initial guess of the unknown maneuver is set to be zero, and we choose $\boldsymbol{\Gamma} = 1 \times 10^5 \times \mathrm{diag}([1, 10, 1])$. Fig. 10 shows the estimated target unknown acceleration (solid black) converge to the real value (dashed line). Obviously, if the target changes its orbit acceleration it will be guaranteed to converge to a new stable estimate like the phenomenon in Fig. 2. Fig. 11 shows the relative distance and sight angle respectively, where the dashed line is the desired value. All the states converge to the desired value after 100 s. The adaptive control acceleration of the chaser spacecraft is shown in Fig. 12. From the above simulation, we notice that this form of adaptive controller is valid for affine unknown parameters that can be applied to more complex missions.

5. Discussion

In this section, we briefly discuss the limitations of our algorithm, some implementation details and other possible variations of this algorithm.

5.1. Limitations of this algorithm

Strong nonlinearity requires a higher-order power series to achieve appropriate precision, thereby increasing the computational burden of our parameterized control method. Accordingly, the assignment operation may wipe out the efficiency advantage

if the expressions are very complicated. Computational complexity is also based on the order and dimensionality of $L_{k,l}$, which is based on the original system. Some complex systems with lower dimensionality use an SDRE method by solving algebraic Riccati equations or Lyapunov equations will be faster.

5.2. Implementation details

1. The solution of the Riccati equation $\boldsymbol{L}$ after parameterization using Eq. (6) is not certain to be a polynomial matrix. Hence, some complex algebraic expressions require a significant computational burden. It will be efficient to transform the algebraic expression to a polynomial using a Taylor expansion if there are complex algebraic expressions in the parameterized control. In examples such as the dynamic system in the LOS frame mentioned in this paper, there are complex trigonometric function computations in parameterized control so that transforming the algebraic expression to a polynomial expression is efficient.

2. We can sometimes remove the terms with small coefficients in the $\boldsymbol{L}_{k,l}$. Parameterized control is not always an accurate expression for a system, as some small coefficients have little influence on control precision. Hence, removing these terms will save computing time.

3. For constructing the algebraic mapping: a_p, b_q in Eq. (5) are not unique. However, the computational precision of our algorithm is not very dependent on the choice of a_p, b_q. Here we provide a general way to construct a_p, b_q: calculating $\boldsymbol{A}(\boldsymbol{x}, \boldsymbol{\epsilon}) - \boldsymbol{A}_0$ and $\boldsymbol{B}(\boldsymbol{x}, \boldsymbol{\epsilon}) - \boldsymbol{B}_0$, we divide the results to scalar algebraic mappings: a_p, b_q and the corresponding constant matrix: $\boldsymbol{A}_p, \boldsymbol{B}_q$.

5.3. Other variations of this algorithm

1. We can expand the Riccati equation, which could also speed up LQR based methods in non-strong nonlinear systems to estimate local control, such as [20].

2. H_2 optimal control involves finding an appropriate controller and minimizing the H_2 norm of its transfer function. With output feedback, H_2 control design is equivalent to solving two Riccati equations for the optimal control and the optimal observer. These two Riccati equations can both be parameterized and solved offline using our method to speed-up online computation.

6. Conclusion

In this paper, a parameterized nonlinear control synthesis technique was developed. The basic framework comes from parameterized SDRE theory. Many similar approximation techniques have been found to solve nonlinear suboptimal control. The approach in this study is to give a parameterized approximately closed-form feedback controller. We have compared with the standard SDRE methods and the $\theta - D$ technique, both of which should solve algebraic Riccati equations or Lyapunov equations online, which is very time-consuming. By constructing the parameterized coefficient matrix in the cost function this method inherits the asymptotic stability in large initial states like the $\theta - D$ technique. In addition, adaptive control has been designed in this parameterized process to offset the unmodeled dynamics.

Application of the parameterized synthesis to two simple benchmark examples and relative motion of a chaser spacecraft with respect to a target was presented in this paper to certify the validity. Under unknown target maneuvering, we apply an adaptive design to estimate the unknown acceleration and to track the target. The result for tracking and rendezvous with a rotating non-cooperative target exhibits good performance since it takes the advantage of efficient computation and adaptive correction capability. In conclusion, this research has packaged the solution of algebraic Riccati equations and Lyapunov equations offline and constructed an algebraic expression for SDRE control, while some new properties and potential variations have been discussed.

Conflict of interest statement

None declared.

Appendix. Proof of Eq. (8)

For the general term, $k + l \leq i$ assume:

$$\boldsymbol{L}_i = \sum_{p=1}^{\bar{p}} \sum_{q=1}^{\bar{q}} a_p^k b_q^l \boldsymbol{L}_{k,l}^{p,q}, \ k + l = i$$

$$\triangle \boldsymbol{A} = \sum_{p=1}^{\bar{p}} a_p(\boldsymbol{\epsilon}) \boldsymbol{A}_p \tag{36}$$

$$\triangle \boldsymbol{B} = \sum_{q=1}^{\bar{q}} b_q(\boldsymbol{\epsilon}) \boldsymbol{B}_q$$

$$\boldsymbol{A}_c = (\boldsymbol{A}_0 - \boldsymbol{B}_0 \boldsymbol{R}^{-1} \boldsymbol{B}_0^T \boldsymbol{L}_0)$$

From the reference [7], we have the following power series, which can be expressed as a set of Lyapunov equations:

$$\boldsymbol{A}_c^T \boldsymbol{L}_i + \boldsymbol{L}_i \boldsymbol{A}_c = -\boldsymbol{L}_{i-1} \triangle \boldsymbol{A} - \triangle \boldsymbol{A}^T \boldsymbol{L}_{i-1} + [\sum_{j=1}^{i-1} \boldsymbol{L}_j \boldsymbol{B}_0 \boldsymbol{R}^{-1} \boldsymbol{B}_0^T \boldsymbol{L}_{i-j}$$

$$+ \sum_{j=0}^{i-1} \boldsymbol{L}_j (\boldsymbol{B}_0 \boldsymbol{R}^{-1} \triangle \boldsymbol{B}^T + \triangle \boldsymbol{B} \boldsymbol{R}^{-1} \boldsymbol{B}_0^T) \boldsymbol{L}_{i-j-1} \tag{37}$$

$$+ \sum_{j=0}^{i-2} \boldsymbol{L}_j \triangle \boldsymbol{B} \boldsymbol{R}^{-1} \triangle \boldsymbol{B}^T \boldsymbol{L}_{i-j-2}], \ i > 0$$

For the 1st order ($i = 1$), we have $\boldsymbol{L}_1 = \sum_{p=1}^{\bar{p}} a(\boldsymbol{\epsilon})_p \boldsymbol{L}_{1,0}^p + \sum_{q=1}^{\bar{q}} b(\boldsymbol{\epsilon})_q \boldsymbol{L}_{0,1}^q$, the sum of different parameters p, q should be linear, so that in order to simplify, in the derivation we assume $\boldsymbol{L}_1 = a\boldsymbol{L}_{1,0} + b\boldsymbol{L}_{0,1}$ for each pair of parameters of p, q such that plugging Eq. (36) into Eq. (37) gives us:

$$\boldsymbol{A}_c^T (a\boldsymbol{L}_{1,0} + b\boldsymbol{L}_{0,1}) + (a\boldsymbol{L}_{1,0} + b\boldsymbol{L}_{0,1}) \boldsymbol{A}_c$$
$$= -a\boldsymbol{L}_0 \boldsymbol{A}_p - a\boldsymbol{A}_p^T \boldsymbol{L}_0 + (a\boldsymbol{L}_{1,0} + b\boldsymbol{L}_{0,1}) \boldsymbol{B}_0 \boldsymbol{R}^{-1} \boldsymbol{B}_0^T \boldsymbol{L}_0 \tag{38}$$

Eq. (38) can be decomposed as the sum of the following two equations:

$$a\boldsymbol{A}_c^T \boldsymbol{L}_{1,0} + a\boldsymbol{L}_{1,0} \boldsymbol{A}_c = -a\boldsymbol{L}_0 \boldsymbol{A}_p - a\boldsymbol{A}_p^T \boldsymbol{L}_0 + a\boldsymbol{L}_{1,0} \boldsymbol{B}_0 \boldsymbol{R}^{-1} \boldsymbol{B}_0^T \boldsymbol{L}_0$$
$$b\boldsymbol{A}_c^T \boldsymbol{L}_{0,1} + b\boldsymbol{L}_{0,1} \boldsymbol{A}_c = b\boldsymbol{L}_{0,1} \boldsymbol{B}_0 \boldsymbol{R}^{-1} \boldsymbol{B}_0^T \boldsymbol{L}_0 \tag{39}$$

Since $ab \neq 0$, then:

$$\boldsymbol{A}_c^T \boldsymbol{L}_{1,0} + \boldsymbol{L}_{1,0} \boldsymbol{A}_c = -\boldsymbol{L}_0 \boldsymbol{A}_p - \boldsymbol{A}_p^T \boldsymbol{L}_0 + \boldsymbol{L}_{1,0} \boldsymbol{B}_0 \boldsymbol{R}^{-1} \boldsymbol{B}_0^T \boldsymbol{L}_0$$
$$\boldsymbol{A}_c^T \boldsymbol{L}_{0,1} + \boldsymbol{L}_{0,1} \boldsymbol{A}_c = \boldsymbol{L}_{0,1} \boldsymbol{B}_0 \boldsymbol{R}^{-1} \boldsymbol{B}_0^T \boldsymbol{L}_0 \tag{40}$$

Thanks to this we may construct the upper Eq. (40), which is a set of Lyapunov equations without any parameters $\boldsymbol{\epsilon}$.

For 2nd order, assuming $\boldsymbol{L}_2 = a^2 \boldsymbol{L}_{2,0} + b^2 \boldsymbol{L}_{0,2} + ab\boldsymbol{L}_{1,1}$ in Eq. (37), we obtain an equation like Eq. (38):

$$\boldsymbol{A}_c^T (a^2 \boldsymbol{L}_{2,0} + b^2 \boldsymbol{L}_{0,2} + ab\boldsymbol{L}_{1,1}) + (a^2 \boldsymbol{L}_{2,0} + b^2 \boldsymbol{L}_{0,2} + ab\boldsymbol{L}_{1,1}) \boldsymbol{A}_c$$
$$= -(a^2 \boldsymbol{L}_{1,0} + ab\boldsymbol{L}_{0,1}) \boldsymbol{A}_p - \boldsymbol{A}_p^T (a^2 \boldsymbol{L}_{1,0} + ab\boldsymbol{L}_{0,1})$$
$$+ (a\boldsymbol{L}_{1,0} + b\boldsymbol{L}_{0,1}) \boldsymbol{B}_0 \boldsymbol{R}^{-1} \boldsymbol{B}_0^T (a\boldsymbol{L}_{1,0} + b\boldsymbol{L}_{0,1})$$
$$+ \boldsymbol{L}_0 (\boldsymbol{B}_0 \boldsymbol{R}^{-1} \boldsymbol{B}_q^T + \boldsymbol{B}_q \boldsymbol{R}^{-1} \boldsymbol{B}_0^T)(ab\boldsymbol{L}_{1,0} + b^2 \boldsymbol{L}_{0,1})$$
$$+ (ab\boldsymbol{L}_{1,0} + b^2 \boldsymbol{L}_{0,1})(\boldsymbol{B}_0 \boldsymbol{R}^{-1} \boldsymbol{B}_q^T + \boldsymbol{B}_q \boldsymbol{R}^{-1} \boldsymbol{B}_0^T) \boldsymbol{L}_0$$
$$+ b^2 \boldsymbol{L}_0 \boldsymbol{B}_q \boldsymbol{R}^{-1} \boldsymbol{B}_q^T \boldsymbol{L}_0 \tag{41}$$

Since $ab \neq 0$, we assume $\boldsymbol{G}_0 = \boldsymbol{B}_0 \boldsymbol{R}^{-1} \boldsymbol{B}_0^T$, $\boldsymbol{G}_1 = \boldsymbol{B}_0 \boldsymbol{R}^{-1} \boldsymbol{B}_q^T + \boldsymbol{B}_q \boldsymbol{R}^{-1} \boldsymbol{B}_0^T$, $\boldsymbol{G}_2 = \boldsymbol{B}_q \boldsymbol{R}^{-1} \boldsymbol{B}_q^T$ and Eq. (41) could decompose as the sum of the following equations:

$$A_c^T L_{2,0} + L_{2,0} A_c = -L_{1,0} A_p - A_p^T L_{1,0} + L_{1,0} G_0 L_{1,0}$$

$$A_c^T L_{0,2} + L_{0,2} A_c = L_{0,1} G_0 L_{0,1} + L_0 G_1 L_{0,1}$$

$$+ L_{0,1} G_1 L_0 + L_0 G_2 L_0 \tag{42}$$

$$A_c^T L_{1,1} + L_{1,1} A_c = -L_{0,1} A_p - A_p^T L_{0,1} + L_{0,1} G_0 L_{1,0}$$

$$+ L_{1,0} G_0 L_{0,1} + L_0 G_1 L_{1,0} + L_{1,0} G_1 L_0$$

For nth order $L_n = a^n L_{n,0} + b^n L_{0,n} + \sum_{i=1}^{n-1} a^{n-i} b^i L_{n-i,i}$, and we have a similar derivation like the first and second procedures used here. Hence the generalized expression that is shown in Eq. (8).

References

[1] T. Çimen, State-dependent Riccati equation (SDRE) control: a survey, in: 17th IFAC World Congress, vol. 41, IFAC, 2008, pp. 3761–3775.

[2] M. Xin, H. Pan, Nonlinear optimal control of spacecraft approaching a tumbling target, Aerosp. Sci. Technol. 15 (2) (2011) 79–89.

[3] D.T. Stansbery, J.R. Cloutier, Position and attitude control of a spacecraft using the state-dependent Riccati equation technique, in: American Control Conference, vol. 3, IEEE, 2000, pp. 1867–1871.

[4] D. Zhang, J. Luo, D. Gao, A novel nonlinear control for tracking and rendezvous with a rotating non-cooperative target with translational maneuver, Acta Astronaut. 138 (2017) 276–289.

[5] A. Flores-Abad, O. Ma, K. Pham, S. Ulrich, A review of space robotics technologies for on-orbit servicing, Prog. Aerosp. Sci. 68 (8) (2014) 1–26.

[6] B. Geranmehr, N.S. Rafee, Nonlinear suboptimal control of fully coupled non-affine six-DOF autonomous underwater vehicle using the state-dependent Riccati equation, Ocean Eng. 96 (6) (2015) 248–257.

[7] A. Wernli, G. Cook, Suboptimal control for the nonlinear quadratic regulator problem, Automatica 11 (1) (1975) 75–84.

[8] M. Xin, A New Method for Suboptimal Control of a Class of Nonlinear Systems, Ph.D. thesis, University of Missouri-Rolla, 2003.

[9] S. Liang, H. Wei, Robust adaptive relative position tracking and attitude synchronization for spacecraft rendezvous, Aerosp. Sci. Technol. 41 (2015) 28–35.

[10] C. Pukdeboon, P. Kumam, Robust optimal sliding mode control for spacecraft position and attitude maneuvers, Aerosp. Sci. Technol. 43 (2015) 329–342.

[11] C. Wei, J. Luo, B. Gong, M. Wang, J. Yuan, On novel adaptive saturated deployment control of tethered satellite system with guaranteed output tracking prescribed performance, Aerosp. Sci. Technol. 75 (2018) 58–73.

[12] L. Zhang, Z. Shifeng, Y. Huabo, Relative attitude and position estimation for a tumbling spacecraft, Aerosp. Sci. Technol. 42 (2015) 97–105.

[13] Y. Sun, C. Li, H. Ling, Adaptive finite-time control for spacecraft to track and point non-cooperative space targets, in: Control and Decision Conference, IEEE, 2017, pp. 6184–6189.

[14] J.R. Cloutier, C.N.D. Souza, C.P. Mracek, Nonlinear regulation and nonlinear h_∞ control via the state-dependent Riccati equation technique, in: International Conference on Nonlinear Problems in Aviation and Aerospace, 1996.

[15] S. Nazari, B. Shafai, Robust SDC parameterization for a class of extended linearization systems, in: American Control Conference, IEEE, 2011, pp. 3742–3747.

[16] A.K. Banerjee, Optimal feedback gains for three-dimensional large angle slewing of spacecraft, J. Guid. Control Dyn. 14 (67) (1991) 1313–1315.

[17] M. Xin, S.N. Balakrishnan, D.T. Stansbery, Nonlinear missile autopilot design with theta-d technique, J. Guid. Control Dyn. 27 (3) (2004) 406–417.

[18] M. Krstić, K.P.V., Control Lyapunov functions for adaptive nonlinear stabilization, Syst. Control Lett. 26 (1) (1995) 17–23.

[19] J. Moore, R. Tedrake, Adaptive control design for underactuated systems using sums-of-squares optimization, in: American Control Conference, IEEE, 2014, pp. 721–728.

[20] A. Perez, R. Platt, G. Konidaris, L. Kaelbling, T. Lozano-Perez, LQR-RRT*: optimal sampling-based motion planning with automatically derived extension heuristics, IEEE Int. Conf. Robot. Autom., vol. 20, IEEE, 2012, pp. 2537–2542.